

In Situ Detection of Adsorbates at Silica/Solution Interfaces by Fourier Transform Infrared Attenuated Total Reflection Spectroscopy Using a Silica-Coated Internal Reflection Element

PETE E. POSTON,* DION RIVERA, RORY UIBEL, and JOEL M. HARRIS †

Department of Chemistry, University of Utah, Salt Lake City, Utah 84112

A silica-coated ZnSe internal reflection element (IRE) was used to acquire attenuated total reflection (ATR) Fourier transform infrared (FT-IR) spectra of ethyl acetate at an *n*-heptane/silica surface. A thin silica film was deposited onto the IRE by withdrawing the substrate from a suspension of fumed silica; upon drying, a durable, porous SiO₂ layer is formed on the IRE that is stable in contact with aprotic solvents. The layer thickness is targeted to be comparable to the depth of penetration of infrared radiation beyond the IRE/film interface. These films were used to investigate the adsorption of ethyl acetate onto silica from *n*-heptane. A multidimensional least-squares fit of the spectroscopic data reveals multiple surface-site energies on the silica surface, as reflected in both the solution concentration dependence of ethyl acetate accumulation on the surface and the frequencies of vibrational modes that shift upon adsorption.

Index Headings: ATR FT-IR; Adsorption; Liquid/solid interfaces.

INTRODUCTION

The surface chemistry of silica impacts many areas of science and technology.¹⁻³ The adsorption and/or binding of molecules to silica surfaces from liquid solution is important in chemical separations and liquid chromatography, chemical modification and passivation of oxide surfaces, and immobilization of catalysts and reagents on high-surface-area supports. To support investigation of these applications, considerable effort has been directed toward the development of *in situ* optical spectroscopies that can be used to observe the behavior of molecules at the silica/solution interface. Fluorescence spectroscopy has been successfully applied to detection of adsorbed⁴⁻⁶ or covalently bound⁷⁻⁹ probes at silica/solution interfaces; the high sensitivity of this technique allows submonolayer surface coverages to be easily detected. Optical absorption (diffuse reflectance) spectroscopy of solvatochromic probes has also been applied to the characterization of C-18 modified silica/solution interfaces.¹⁰ The high surface area and optical transparency of silica materials have allowed the use of Raman spectroscopy to detect both adsorbates^{11,12} and surface-bound alkyl ligands^{13,14} on silica. Surface-enhanced Raman spectroscopy has been successfully employed to observe C-18 ligands attached to a silica sol-gel coating bound to a roughened-silver surface.^{15,16}

Internal reflection infrared spectroscopy¹⁷ can also be used to observe *in situ* vibrational spectra of adsorbed or bound molecules at solid/liquid interfaces.^{18,19} For investigating the chemistry of covalently binding molecules to silica surfaces, elemental silicon internal reflection elements (IREs) were surface oxidized in a furnace to create a thin layer of amorphous silica for studies of silane binding to SiO₂ surfaces.^{20,21} While this approach allows *in situ* detection of adsorbed and bound molecules at silica surfaces, there are several drawbacks that limit its utility. First, the silicon IRE limits the transmission of long-wavelength infrared radiation and confines measurements to frequencies higher than 1600 cm⁻¹. In addition, sensitivity for detecting molecules on the surface is reduced by decay of the evanescent wave through the silica layer to reach molecules at the silica/solution interface.

In this work, we address both the limited spectral range allowed by a silicon IRE for these measurements and the sensitivity of detecting molecules at a flat silica surface. We have been able to deposit a thin layer of colloidal silica particles onto a ZnSe IRE to provide a high-surface-area substrate for attenuated total reflection Fourier transform infrared (ATR FT-IR) detection of molecules at silica/solution interfaces. Inspiration for this approach was initially derived from a study²² in which the binding of TiO₂ colloid particles onto an IRE allowed the detection of adsorbed anions (sulfate, acetate) at the TiO₂/water interface. The method was also adapted²³ to other oxides (ZrO₂ and Al₂O₃) and used to detect coordinating ligands (catechol, 8-hydroxyquinoline, acetylacetonate) at metal oxide surfaces. In a more recent paper, the deposition of a sol-gel silica film coating onto a silicon IRE was reported;²⁴ the silica surface was modified with C-8 alkyl ligands and used to detect benzonitrile at low concentrations in solution by their accumulation onto the high-surface-area, hydrophobic sol-gel coating. As has been shown by thin (nonporous) film modification of IREs,^{25,26} surface coatings should allow a variety of surface chemistries to be investigated with internal reflection spectroscopy while using a broad-band IRE to open up the spectral window for infrared absorption measurements throughout the entire mid-infrared range. The porous nature of a particulate film can additionally provide an enhanced surface area for detection of submonolayer species.

In the present study, we have modified surfaces of a broad-band ZnSe internal-reflection element with particulate silica films. A thin film of silica was deposited onto the IRE by withdrawing the substrate from a suspension

Received 29 May 1998; accepted 5 August 1998.

* Current address: Division of Natural Science and Mathematics, Western Oregon University, 345 N. Monmouth Ave., Monmouth, OR 97361.

† Author to whom correspondence should be sent.

of the sol; upon drying, a network of siloxane and hydrogen bonds between silanol groups holds the precipitate in place. This approach has led to a porous SiO_2 layer that is stable in contact with aprotic solvents. The film thickness is targeted to be comparable to the depth of penetration of the infrared evanescent wave beyond the IRE/gel interface. We have employed these silica films to investigate the adsorption of ethyl acetate onto silica from *n*-heptane; on the basis of chromatographic data, adsorption of ethyl acetate onto silica was reported by Scott and Kucera²⁷ to exhibit nonlinear isotherm behavior. Application of a silica-coated IRE has allowed us to measure *in situ* infrared spectra of the adsorbate and its dependence on the solution concentration. A multidimensional least-squares fit of the data to an appropriate isotherm model reveals multiple surface-site energies, as reflected in both the solution-concentration dependence of surface accumulation and corresponding frequencies of vibrational modes that shift upon adsorption.

EXPERIMENTAL

Materials. Solutions of ethyl acetate in *n*-heptane were prepared with concentrations ranging from 5 to 200 mM. HPLC-grade 2-propanol and reagent-grade *n*-heptane were obtained from Fisher; ethyl acetate was acquired from OmniSolv; these solvents were used as received.

Fumed silica (Cabosil, HS-5, 5 nm particle diameter, 250 m²/g) was deposited onto a cylindrical ZnSe IRE (Axiom) (see Fig. 1) by withdrawing the substrate from a 1% (w/v) suspension of the particles in 2-propanol. At a withdrawal rate of 1 cm/s, the adherent suspension layer should be approximately 16 μm thick (prior to solvent evaporation) on the basis of the viscosity, density, and surface tension of the suspension.²⁸ Between dips, the solvent was allowed to evaporate, and then the IRE was immersed and withdrawn again for a total of 10 to 15 dips. The silica film thickness was determined from the infrared absorption and mass of a film deposited under identical conditions onto a flat ZnSe window. The films appear to be uniform by visual inspection; they are scattering at visible wavelengths due to their porosity.

The fumed silica used in the present study differs from the precipitated silica which Scott and Kucera initially employed in their investigations of adsorption mechanisms;²⁷ the latter material has $\approx 8 \mu\text{M}/\text{m}^2$ of surface OH groups with strongly hydrogen-bonded water associated with the surface.¹ Fumed silica differs from this surface in that the surface OH groups are at much lower density ($\approx 1 \mu\text{M}/\text{m}^2$), and the material is less hydrophilic (less surface water is present). These differences, however, should make a difference only in the relative amount of adsorbate observed in the detection volume as both surfaces have the same sites that are thought to interact with adsorbate, namely, silanols and water.^{29,30} In addition, Scott and Kucera did a second study on a silica that had been heated to sufficiently high temperatures to remove water and vicinal silanols;³¹ this surface is similar to fumed silica, and it produced the same isotherm behavior as the more hydrated material. Thus, while the silica surfaces are not identical, the fumed-silica film should be sufficiently similar to a chromatographic silica gel to ensure that the experimental results can be compared.

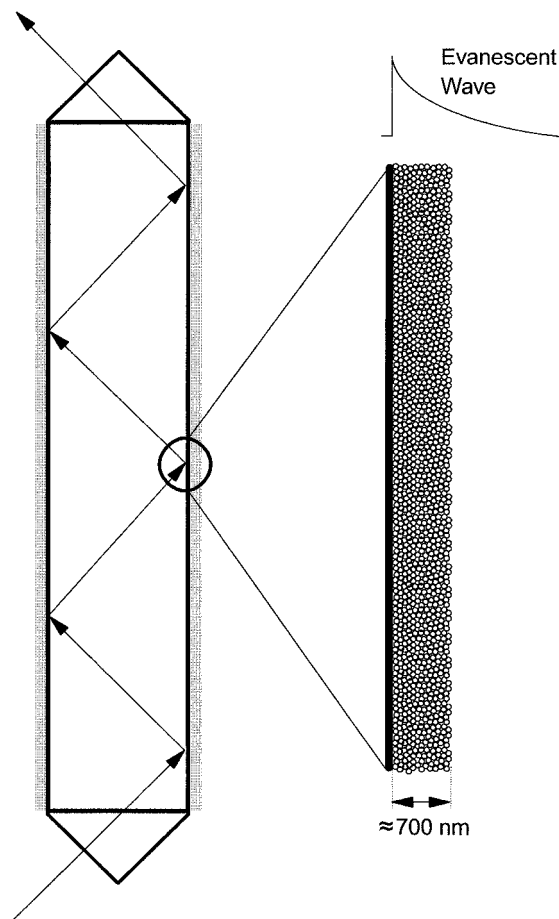


FIG. 1. Silica-coated internal reflection element. A cylindrical ZnSe IRE is dip-coated in a fumed-silica suspension to deposit a ≈ 700 nm porous silica film for interfacial absorption measurements. The film thickness is chosen to be comparable to the sampling depth of the evanescent wave.

Infrared Absorption Spectroscopy. All spectra were acquired with the use of a Bruker Model 66V FT-IR configured with a mercury-manganese-tellurium (MMT) detector and Glowbar (MIR) source. Each spectrum was an average of 500 to 1000 scans, recorded with a resolution of 4 cm^{-1} and an aperture setting of 12 mm. A Mertz phase correction mode was used along with a trapezoidal apodization function. A single-beam spectrum of the uncoated IRE was taken as the reference spectrum.

An Axiom Model TNL-130A standard tunnel cell was used with a bare or silica-coated, $\frac{1}{4}$ in. \times $3\frac{1}{4}$ in., cylindrical, ZnSe IRE. A Gilson peristaltic pump was used to flow sample solutions through the cell at a rate of ≈ 1.0 mL/min. The solution was flowed for approximately 5 min between changes in concentration to allow equilibration of adsorbate on the surface.

Data Analysis. Spectra were background corrected by acquiring a spectrum of the silica-coated IRE with only solvent flowing through the cell. This unscaled spectrum was subtracted from all spectra containing adsorbate. This procedure removed silica and solvent bands from the adsorbate spectra.

Modeling of spectroscopic isotherm data was performed by using Matlab 4.0 on a 486DX2-66 PC. To resolve the adsorbate and solution-phase infrared spectra,

we acquired a series of ATR FT-IR spectra vs. ethyl acetate concentration in solution. The spectra are placed in columns of a matrix \mathbf{D} with dimensions r rows by c columns. Each column contains a spectrum at a given solution concentration, where the row index i is for the infrared frequency and the column index j is for the samples prepared at different adsorbate concentration. Assuming Beer's law is obeyed and the infrared absorption of the components are independent and additive, the absorption for wavenumber i and sample composition j is the sum of the components, $k = 1$ to n , at the interface:

$$d_{i,j} = \sum_{k=1}^n a_{i,k} c_{k,j} \quad (1)$$

where $a_{i,k}$ is the absorptivity of the k th component at the i th wavenumber, and $c_{k,j}$ is the interface concentration of the k th component at the j th solution condition. Equation 1 can be expressed in matrix form:

$$\mathbf{D} = \mathbf{A}\mathbf{C} \quad (2)$$

where \mathbf{A} is an $r \times n$ matrix containing spectra of the n isolated components in the system, and \mathbf{C} is an $n \times c$ matrix containing the interface concentration variation of these components.

Resolution of the spectra in \mathbf{D} into resolved components \mathbf{A} and \mathbf{C} is accomplished by modeling the concentration dependence of \mathbf{C} , where one row is proportional to the solution-phase concentration of the adsorbate and one or more rows are modeled by an adsorption isotherm. Given a model for the interface concentrations, $\hat{\mathbf{C}}$, a least-squares estimate for the component spectra, $\hat{\mathbf{A}}$, can be obtained by a right pseudoinverse of $\hat{\mathbf{C}}$.^{32,33}

$$\hat{\mathbf{A}} = \mathbf{D}\hat{\mathbf{C}}^T(\hat{\mathbf{C}}\hat{\mathbf{C}}^T)^{-1} \quad (3)$$

The nonlinear parameters (β 's) for the isotherm model for $\hat{\mathbf{C}}$ are varied by using a Nelder–Mead Simplex algorithm³⁴ to achieve a least-squares fit of the data by minimizing the sum of the squares of the residuals, $\mathbf{R}^T\mathbf{R}$, where $\mathbf{R} = \mathbf{D} - \hat{\mathbf{A}}\hat{\mathbf{C}}$. The optimum was checked by plotting the squared residuals vs. both nonlinear parameters to verify that it was a global minimum.

RESULTS AND DISCUSSION

Film Deposition and Characterization. To obtain a high sensitivity to adsorbates, the silica layer deposited onto the IRE should have a thickness that is greater than or equal to the depth penetration of the evanescent wave into this layer. This condition allows the three-layer interface (IRE/silica/solution) to be simplified to a two-layer optical system. Throughout the mid-infrared region, the refractive indices of both alkane solvents³⁵ and amorphous silica³⁶ are well below that of ZnSe, so that the evanescent wave originates at the ZnSe/silica interface. At a 45° incident angle, the depth of penetration of the evanescent wave is comparable to the average layer thickness sampled by unpolarized radiation,¹⁷ which is relevant to this case since a cylindrical IRE has been shown to scramble any polarization of the incident radiation from the interferometer.³⁷ The depth of penetration of the evanescent wave (where its intensity drops by 1/e²) is given by¹⁷

$$d_p = \frac{\lambda}{4\pi n_1(\sin^2\theta - (n_2/n_1)^2)^{1/2}} \quad (4)$$

where n_1 and n_2 are the refractive indices of the ZnSe IRE (2.42) and the silica gel/heptane phase (≈ 1.3), respectively, and $\theta = 45^\circ$ is the angle of incidence. The expected depth of penetration varies with wavelength, from approximately 400 nm at 1800 cm⁻¹ to 700 nm at 1000 cm⁻¹.

The thickness of the silica layer deposited onto the internal reflection element was estimated by coating a circular ZnSe window, dipped 10 times in the 1% weight/volume suspension of fumed silica in 2-propanol, using the substrate-withdrawal coating method described in the Experimental section. The outside edge of the window was wiped free of silica, and the coated window was then heated in a drying oven at 120 °C for 1 h to drive off excess solvent, cooled in a desiccator, and weighed. With 10 dips, the uptake of silica by the ZnSe substrate per unit area was found to be 8.8×10^{-5} g/cm², corresponding to a silica (only) thickness of 240 nm based on the density of fumed silica (2.2 g/cm³). The infrared absorption of two 5-dip coated films on both sides of the ZnSe substrate was also measured, and the transmittance was found to be $T = 0.9602$ and 0.9700 at 840 and 850 cm⁻¹, respectively, where the extinction coefficient of amorphous SiO₂ has been measured by thin-film transmittance³⁶ to be $k_{\text{abs}} = 0.17$ and 0.12 , respectively. The total silica thickness for the two films was determined from these results by using the relation³⁸ $t = -\ln(T)\lambda/4\pi k_{\text{abs}} = 230$ nm, which is comparable to the silica mass thickness for a single 10-dip film.

These results would appear to indicate that evanescent wave would penetrate beyond the silica film; however, both the mass- and absorbance-thickness estimates are based on the density and extinction coefficient of a nonporous, fused-silica film and thus report the thickness of the solid SiO₂ fraction of the porous film. The actual film density and extinction coefficient are reduced by film porosity, which depends on how the 5 nm fumed-silica particles pack. If the aggregation is a maximum, hexagonal closed-packed structure with coordination number of 12, the film density would be reduced by 26%;¹ more likely structures would exhibit lower coordination numbers—6 for cubic or 4 for tetragonal—which would decrease the density by 48% and 67%, respectively.¹ The actual film, therefore, should exhibit about half the density of fused silica and twice the SiO₂ mass thickness. On the basis of these results and as an assurance that the evanescent wave does not sample well beyond the boundary of the porous film, 15-dip coats of the 1% silica suspension were deposited onto the internal reflection element for adsorption studies, which provides a total film thickness estimated to be ≈ 700 nm, which is comparable to the maximum depth of penetration of the evanescent wave at 1000 cm⁻¹.

The enhancement of surface area provide by a silica particle layer over that of a thin, flat nonporous film on the IRE is considerable. The 5 nm fumed silica has a specific surface area of 250 m²/g; from the mass of the deposited layer (≈ 0.132 mg/cm² for a 15-dip film), the silica surface area in the porous film should be 0.033 m² per cm² of the IRE surface. The silica film significantly

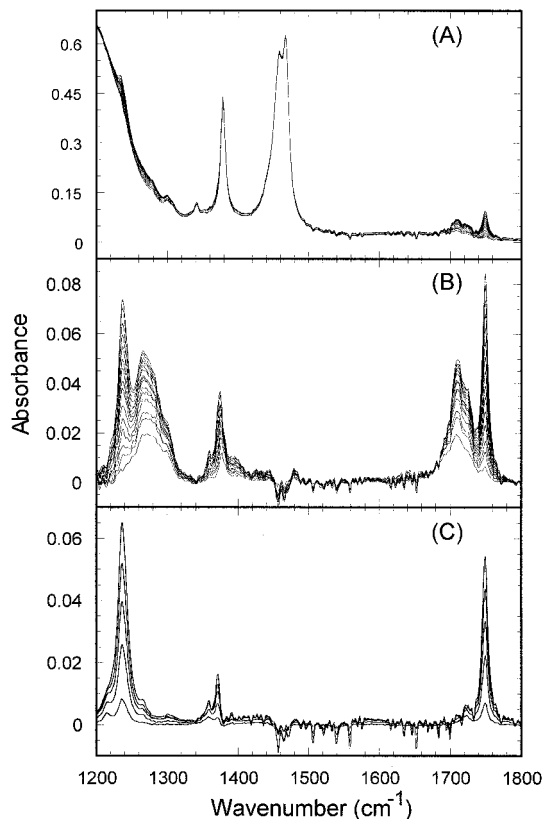


Fig. 2. ATR FT-IR spectra of ethyl acetate in *n*-heptane. (A) Silica-coated IRE in contact with *n*-heptane solutions containing 5.1 to 77 mM ethyl acetate. (B) Difference spectra derived from (A) where a spectrum of *n*-heptane in contact with the silica-coated IRE has been subtracted. (C) Uncoated ZnSe IRE in contact with *n*-heptane solutions containing 10.2 to 51 mM ethyl acetate.

enhances the interfacial area, by as much as a factor of 330 times relative to the IRE surface.

Adsorption of Ethyl Acetate to Silica Surfaces. The silica-coated IRE was mounted in a flow-through tunnel cell and exposed to a series of *n*-heptane solutions containing ethyl acetate in the range of 5.1 to 77 mM. The resulting ATR spectra (referenced to a background spectrum of the uncoated IRE) are plotted in Fig. 2A. The raw spectra are dominated by *n*-heptane bands at 1380 and 1460 cm^{-1} and by the shoulder of a large silica peak below 1300 cm^{-1} . Weak absorption by ethyl acetate is observed around 1250 cm^{-1} and 1750 cm^{-1} , which increases with increasing solution concentration.

The absorption spectra of the ethyl acetate, both in solution and adsorbed to the silica surface, are more apparent in difference spectra (Fig. 2B) that are generated by subtracting an unscaled spectrum of the silica-coated IRE in contact with *n*-heptane solvent. The silica and solvent bands are eliminated in the difference spectrum, with the exception of the stronger *n*-heptane band at 1460 cm^{-1} , which produces a small, negative-going peak in the difference spectrum, with an amplitude that is proportional to the concentration of ethyl acetate in solution. This negative-going *n*-heptane peak is also present in the solution spectrum even when no silica is present on the IRE (Fig. 2C). Therefore, this negative-going band likely arises from a simple displacement of *n*-heptane from the

solution in the evanescent wave volume by the increasing ethyl acetate concentration.

To identify the vibrational features of ethyl acetate adsorbed to the silica surface, we acquired comparison spectra of the solute in *n*-heptane with an uncoated ZnSe IRE, and the results are plotted in Fig. 2C. Comparison of Figs. 2B and 2C reveals the presence of adsorbate bands growing in adjacent to free-solution bands. On the basis of previous assignments from the literature,^{39,40} a qualitative interpretation of the spectra follows. The prominent peak at 1750 cm^{-1} is due to the carbonyl stretch of solution-phase ethyl acetate (Fig. 2C). The shoulder at 1710 cm^{-1} arises from the adsorbate C=O stretch, since this peak disappeared when 2-propanol, a more polar molecule that interacts with silica more strongly than ethyl acetate,⁴¹ is introduced into the solution that displaces adsorbed ethyl acetate from the surface. The fact that the 1710 cm^{-1} adsorbate peak is found at a lower frequency indicates that electron density is being withdrawn from the bond due to hydrogen bonding interactions with surface silanols and/or surface water.

The band that peaks at 1240 cm^{-1} is due to the C–C–O stretch of solution-phase ethyl acetate. Specifically, the 1240 cm^{-1} band is assigned to the strong $\text{H}_3\text{C–C–O}$ stretch^{39,40} where the second carbon is part of the carbonyl group; the adsorbate C–C–O stretching frequency for this same vibrational mode occurs at 1270 cm^{-1} . The observation that the C–C–O vibration is shifted to higher frequency indicates that the bond is strengthened, which is consistent with the weakening of the carbonyl bond. While electron density is being removed from the carbonyl bond and directed toward the surface, electron density is shifting into the C–C–O bonds adjacent to the carbonyl. Overall, these band shifts indicate a strong dipolar interaction between the carbonyl group of ethyl acetate with the –OH groups on the surface.

The infrared absorbance from solution-phase ethyl acetate at a silica-coated vs. an uncoated IRE can be compared in Figs. 2B and 2C. The maximum absorbances of the 1750 and 1240 cm^{-1} solution-phase bands in the spectra are comparable: $A_{\text{max}} \approx 0.06\text{--}0.07$, for the highest ethyl acetate concentrations in each experiment, 77 mM for the coated IRE and 51 mM for the uncoated IRE. The 34% lower sensitivity for solution-phase species when the coating is present on the IRE shows that the silica coating excludes solvent from a significant fraction of the evanescent wave volume.

Interfacial ATR spectra were also collected over a 20-fold higher concentration range than reported in Fig. 2 in order to investigate the saturation behavior of the isotherm. At these higher concentrations, shifting of the solution band frequencies was observed; the peak frequency of the C=O band at 1750 cm^{-1} shifted approximately 2 cm^{-1} toward lower frequency, and a smaller shift was observed for the C–C–O band at 1240 cm^{-1} . To test whether this shifting arises from an adsorbed bilayer exhibiting solution-like band frequencies, we collected the spectra at the higher ethyl acetate concentrations without any silica gel coating on the IRE, and similar band shifting was observed. When the series of solution spectra were acquired in a conventional, thin-pathlength (50 μm) transmission flow cell, no peak shifting could be detected. We ascribe the shifting of these bands, therefore, to ef-

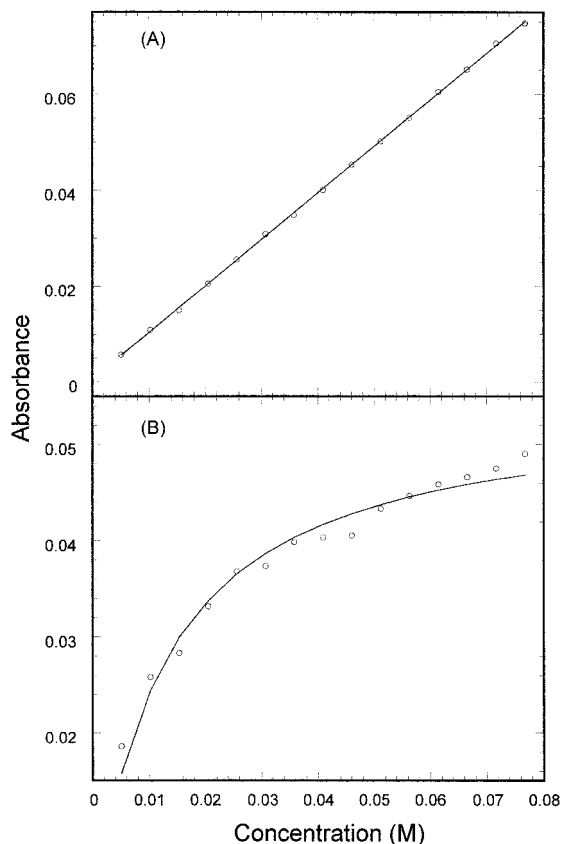


FIG. 3. Infrared absorption of ethyl acetate at a silica interface vs. solution concentration. (A) Absorbance at 1240 cm^{-1} from solution-phase ethyl acetate varies linearly with the concentration. (B) Absorbance at 1274 cm^{-1} from silica-adsorbed ethyl acetate follows the form of an adsorption isotherm (solid line).

fects of anomalous dispersion on the sampling depth of the evanescent wave.^{37,42} When the ethyl acetate solution concentration is large ($>500\text{ mM}$), its refractive index contributes significantly to the index of the solution; in the vicinity of strong absorption bands, the resulting anomalous dispersion can give rise to changes in sampling depth with wavelength that lead to apparent shifts in the band shape. Thus, to interpret the absorption spectra, without resorting to a Kramers–Kronig analysis, requires that changes in the interfacial absorbance be kept small so that the wavelength-dependent depth of penetration does not change with the solution composition.

Ethyl Acetate Adsorption Isotherms. The absorbance of ethyl acetate at several infrared frequencies was plotted vs. the solution concentration to investigate the accumulation of adsorbate at the silica/solution interface. Example results are shown for data from C–C–O bands in the $1240\text{--}1280\text{ cm}^{-1}$ region in Fig. 2B. The absorbance at 1240 cm^{-1} (Fig. 3A) grows linearly with the concentration in solution; this observation agrees with the assignment of this band to a solution-phase species based on comparison with spectra collected at an uncoated IRE as well as a thin-path transmission cell. A linear response was also observed for absorbance at 1750 cm^{-1} assigned to the C=O stretching mode of solution-phase ethyl acetate.

The amplitudes of solution-like ethyl acetate bands were analyzed quantitatively in order to test for the ac-

cumulation of any surface excess in this interface population. In the analysis of the nonlinear chromatographic retention of ethyl acetate on silica,²⁷ Scott and Kucera proposed the formation of a weakly retained bilayer at the interface between the solution and silica-adsorbed ethyl acetate.^{27,31} The infrared spectrum of ethyl acetate in such a bilayer, where molecules would reside at the interface between ethyl acetate and *n*-heptane, should be indistinguishable from ethyl acetate in free solution since frequencies of ethyl acetate C–C–O and C=O modes are the same in the neat liquid and in dilute *n*-heptane solution. To identify any surface excess in the solution-like ethyl acetate absorption, we made a quantitative comparison to free-solution spectra acquired by using an IRE without the silica gel coating. To correct for loss of the solution volume displaced by the silica within the evanescent wave, we ratioed the measured ethyl acetate absorption to a nearby solvent peak at 1460 cm^{-1} , which also corrects for any changes in sensitivity (number of reflections) in the ATR measurement. The results showed no evidence for a surface excess of solution-like ethyl acetate at the interface; for example, absorbance at 1750 cm^{-1} ratioed to the solvent peak increased linearly with solution concentration of ethyl acetate with a slope for the silica-coated IRE that was indistinguishable from the slope with the bare IRE. For absorbance measured at 1240 cm^{-1} , a somewhat greater slope was observed with the bare IRE, but again no evidence of additional solution-like ethyl acetate in the interfacial absorbance data—which runs counter to the bilayer hypothesis of Scott and Kucera.^{27,31} This result leaves open the question of how to account for the nonlinear isotherm behavior observed in chromatographic data on this system.

Infrared absorption by the silica-adsorbed ethyl acetate, in wavenumber regions where the solution-phase absorption is weak, follows the expected form of an adsorption isotherm as shown in Fig. 3B for absorbance monitored at 1274 cm^{-1} . These data are fit to a simple Langmuir isotherm:⁴³

$$\theta = \frac{\beta C}{1 + \beta C} \quad (5)$$

where θ is the fractional surface coverage of the adsorbate, C is its concentration in solution, and β is the equilibrium constant for adsorption. A least-squares fit of the data in Fig. 3B to Eq. 5 does a reasonable job in describing the accumulation of adsorbate at the silica surface, where the best-fit equilibrium constant is 76 M^{-1} . Some nonrandomness is apparent in the residuals, however, especially at higher concentrations; the residuals fail a run test⁴⁴ at 85% confidence. More importantly, the best-fit equilibrium constant depends on the infrared frequency at which absorbance is monitored. Indeed, there is a systematic trend in the apparent equilibrium constant with wavenumber for both adsorbate bands; for the C–C–O band at 1274 cm^{-1} , β is 76 M^{-1} (Fig. 3B), while at 1287 cm^{-1} , β is 100 M^{-1} and at 1300 cm^{-1} , β is 133 M^{-1} . For the C=O band, at 1688 cm^{-1} , β is 399 M^{-1} , while at 1720 cm^{-1} , β is 65 M^{-1} . These spectroscopic results, therefore, indicate a dispersion in adsorption interactions of ethyl acetate with the interface surface, where more strongly adsorbed molecules exhibit higher frequency

C–C–O stretching and lower frequency C=O stretching. These shifts are in the same direction as the changes in frequency of these two modes for the adsorbate compared to solution-phase ethyl acetate, as discussed above.

A dispersion in adsorption free energy (equilibrium constant) and the corresponding spectra of the adsorbate can be challenging to model.¹² When ions are adsorbed or when adsorption leads to formal charge or proton transfer between the surface and the adsorbate, dispersion in adsorption energy with coverage can be described by a Frumkin isotherm^{45,12} that accounts for the electrostatic interactions between adsorbates on the surface. Ethyl acetate adsorption to silica should not exhibit strong acid–base interactions so that a Frumkin model would not be appropriate; indeed, the data in Fig. 2B were fit to a Frumkin isotherm, but the resolved spectra showed negative intensity regions and were not realistic. An alternative explanation of the nonlinear isotherm behavior of ethyl acetate adsorption has been proposed by Synder and Poppe²⁹ on the basis of rearrangement (delocalization) of the adsorbate layer at high coverages; the resulting response is similar in form to a Frumkin isotherm and was not successful in fitting these results.

Since there are distinct populations of hydrogen-bonding groups on the silica surface including silanols (isolated, geminal, vicinal^{1,2} that exhibit differences in hydrogen bonding strength) and adsorbed water, where ethyl acetate could act to lower the interfacial tension with the *n*-heptane solvent, one would expect to observe a dispersion in adsorption free energies. The appropriate model for adsorption to discrete, noninteracting sites is a multiple Langmuir isotherm, the simplest form of which would hypothesize two discrete surface sites for adsorption. The total surface coverage, θ_{total} , is the sum of two independent Langmuir equilibria:

$$\begin{aligned}\theta_{\text{total}} &= \theta_1 + \theta_2 \\ &= \frac{\theta_1^{\text{max}}\beta_1 C}{1 + \beta_1 C} + \frac{\theta_2^{\text{max}}\beta_2 C}{1 + \beta_2 C}\end{aligned}\quad (6)$$

where θ_1^{max} and θ_2^{max} are the fraction of the surface sites of type 1 and 2 having exhibiting equilibrium constants, β_1 and β_2 , respectively.

The ethyl acetate concentration-dependent infrared reflection/absorption spectra in Fig. 2B were fit to a simple two-Langmuir model for the adsorbed population, together with a component that is linear with concentration to capture the solution-phase ethyl acetate response. The entire spectral range of Fig. 2 was fit simultaneously by using nonlinear least-squares to optimize the two parameters, β_1 and β_2 , and linear least-squares (Eq. 3) to resolve spectra of the three components. The two-site model improved the quality of fit of the data compared to a single Langmuir isotherm; the residual error was reduced by 20%, and the improvement in fit was significant at >95% confidence according to an *F*-test. The best fit values of the two adsorption equilibrium constants found by fitting the entire 1200 to 1800 cm^{-1} spectral range were $\beta_1 = 830 \text{ M}^{-1}$ for the stronger adsorption site, and $\beta_2 = 57 \text{ M}^{-1}$ for the weaker site. To determine whether both vibrational modes report comparable adsorption behavior, we separately fit the C=O spectral region from 1650 to 1800 cm^{-1} with good agreement, where $\beta_1 = 840 \text{ M}^{-1}$

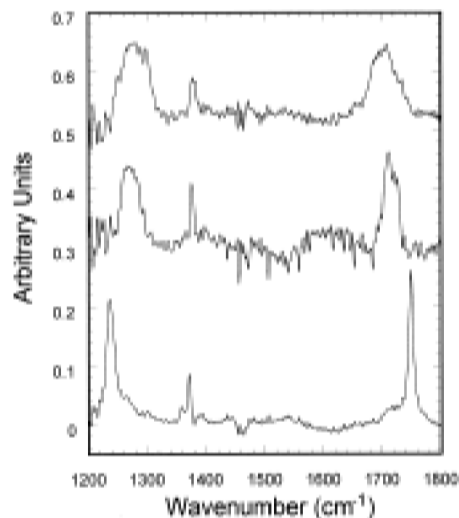


FIG. 4. Component spectra resolved by fitting ATR FT-IR spectra of ethyl acetate to a two-Langmuir adsorption model. (Top) Strongly adsorbed component spectrum, $\beta_1 = 830 \text{ M}^{-1}$; (middle) weakly adsorbed component spectrum, $\beta_2 = 57 \text{ M}^{-1}$; (bottom) solution-phase component, linear with concentration. Spectra are normalized to the same area; the top two spectra are offset by 0.3 and 0.5 units for plotting.

and $\beta_2 = 68 \text{ M}^{-1}$; when the C–C–O region from 1200 to 1350 cm^{-1} was separately analyzed, the equilibrium constants were of similar magnitude but somewhat smaller, $\beta_1 = 580 \text{ M}^{-1}$ and $\beta_2 = 38 \text{ M}^{-1}$. The C=O spectral region appears to have greater influence on the fit of the entire spectral range, probably because of the better resolution of the component spectra in this region (see Fig. 4).

A significant difference in adsorption energy is reflected in the two equilibrium constants, which differ by more than an order of magnitude; the difference in adsorption free energy for these two sites is given by $\Delta(\Delta G_{\text{ads}}) = -RT \ln(\beta_2/\beta_1) = -6.7 \text{ kJ/mol}$. One would expect the vibrational spectra of ethyl acetate adsorbed to sites at such different free energies to be distinguishable. To test this expectation, we show the spectra resolved by least-squares fitting (Eq. 3) of the infrared absorption data to a two-Langmuir plus linear model in Fig. 4. The spectra of the components are unique, with no significant negative absorbance; the solution-phase spectrum resolved from these data is indistinguishable from that measured at a bare ZnSe IRE (Fig. 2C). The C–C–O and C=O band frequencies for the spectra of the two adsorbed components follow the expected variation with adsorption free energy. The more strongly adsorbed component exhibits a C–C–O stretching vibration at a higher frequency and a C=O stretch at a lower frequency, in comparison to the weakly adsorbed component. Both adsorbate spectra are shifted in these directions in comparison to solution-phase ethyl acetate, as discussed in the previous section. One final spectral feature should be noted: the ethyl acetate band at 1375 cm^{-1} arises from symmetric deformation of the methyl group adjacent to the carbonyl group. No direct surface interaction would be expected between a methyl group and surface sites, but apparently this band is sensitive to adsorption because of its electronic coupling to the carbonyl group. This peak follows the same frequency trend as the C–C–O vibration, shifting toward higher frequency upon adsorption by an

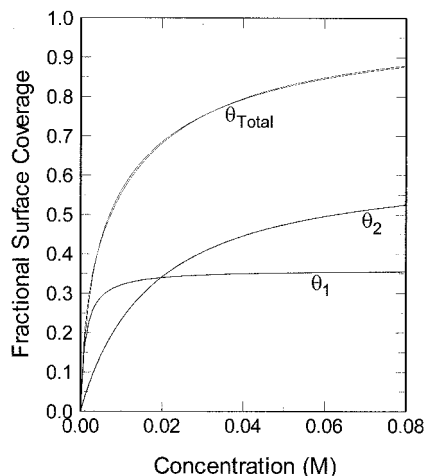


FIG. 5. Surface coverages of ethyl acetate onto two surface sites on silica. The total surface coverage is also plotted, together with a best fit to a bilayer isotherm model.

amount that increases with strength of the adsorption equilibrium.

The interpretation of the adsorption results is summarized as follows: Ethyl acetate encounters two distinguishable adsorption sites on the silica surface that exhibit significant differences in hydrogen-bonding activity. The stronger adsorption site produces a greater perturbation of the C–C–O and C=O stretching frequencies upon adsorption, which is also reflected in a 15-fold greater adsorption equilibrium constant. The relative populations of these two surface sites can be estimated from the amplitude of the infrared absorption of the two adsorbed component spectra, assuming that the oscillator strengths of the bands are not significantly different for molecules adsorbed to these two sites. From the two factors used to normalize the spectra in Fig. 4, the relative populations of stronger and weaker sites are $\theta_1^{\max} = 0.36$ and $\theta_2^{\max} = 0.64$, respectively.

These results can be used to explain the nonlinear adsorption isotherm reported from chromatographic retention of ethyl acetate on silica surfaces²⁷ and demonstrate how the accumulation of this adsorbate at the surface could have easily been mistaken for a bilayer isotherm; recall that there was no spectroscopic evidence (see above) for an ethyl acetate bilayer previously proposed to model the chromatographic results.²⁷ On the basis of the values of β_1 , β_2 , θ_1^{\max} , and θ_2^{\max} determined from the spectroscopic results, accumulations of ethyl acetate at both surface sites, θ_1 and θ_2 , are estimated by Eq. 6 and are plotted in Fig. 5 along with the total surface coverage, θ_{total} . Also plotted in Fig. 5 is the best fit of the total coverage to the bilayer isotherm model. As can be seen in these results, the bilayer isotherm provides an equally good fit of the total accumulation of adsorbate vs. solution concentration. In the absence of any spectroscopic evidence about the chemical form of the adsorbate at the interface, there is no indication from the dependence of surface coverage on solution concentration that a bilayer isotherm is not an appropriate model for this system. This result points out the power of *in situ* monitoring of adsorbate spectra where the chemical forms of an adsorbate, as well as their relative coverage, can be determined.

The one issue that is not resolved by these data is the nature of the two surface sites on silica that are responsible for the dispersion in adsorption energies. Preliminary results obtained by monitoring the adsorption in the O–H stretching region suggest discernible roles by both silanol groups and surface-adsorbed water in retaining ethyl acetate at the silica surface. Fumed silicas, like those used in the present study, have a meager surface density of silanol groups when compared to precipitated silicas,¹ which makes the production of high signal-to-noise (S/N) silanol spectra challenging in fumed-silica films. We have recently adapted the dip-coating method to deposit precipitated sol-gel silica layers onto germanium IREs. We are presently using these precipitated films (which are also stable in protic solvents) to investigate the O–H stretching response to adsorption of molecules at the silica/solution interface to ascertain the chemical origins of the adsorption site energetics.

CONCLUSION

We have used a particulate silica film deposited on the surface of a broad-band ZnSe internal-reflection element to investigate the adsorption of ethyl acetate onto silica from *n*-heptane. The nonlinear isotherm exhibited by ethyl acetate adsorption onto silica was found to be due to a dispersion in surface-site energies and not due to the formation of an adsorbed bilayer. Application of the silica-coated IRE allows sensitive measurement of *in situ* adsorbate infrared spectra and their dependence on solution concentration. A multidimensional least-squares fit to an appropriate isotherm model can be used to resolve concentration-dependent data into component spectra of each interfacial species.

ACKNOWLEDGMENTS

This work was supported by grants from the National Science Foundation (CHE95-10312) and the U.S. Department of Energy (DE-FG03-93ER14333).

1. R. K. Iler, *The Chemistry of Silica* (John Wiley and Sons, New York, 1979).
2. K. Ungar, *Porous Silica* (Elsevier Scientific, Amsterdam, 1979).
3. C. J. Brinker and G. W. Scherer, *Sol-Gel Science* (Academic Press, San Diego, California, 1989).
4. J. Stahlberg and M. Almgren, *Anal. Chem.* **57**, 817 (1985).
5. J. W. Carr and J. M. Harris, *Anal. Chem.* **58**, 626 (1986).
6. J. W. Carr and J. M. Harris, *Anal. Chem.* **59**, 2546 (1987).
7. C. H. Lochmüller, D. B. Marshall, and D. R. Wilder, *Anal. Chim. Acta* **130**, 31 (1981).
8. C. H. Lochmüller, D. B. Marshall, and J. M. Harris, *Anal. Chim. Acta* **131**, 263 (1981).
9. C. H. Lochmüller, A. S. Colborn, M. L. Hunnicutt, and J. M. Harris, *J. Am. Chem. Soc.* **106**, 4077 (1984).
10. J. L. Jones and S. C. Rutan, *Anal. Chem.* **63**, 1318 (1991).
11. S. F. Simpson and J. M. Harris, *J. Phys. Chem.* **94**, 4649 (1990).
12. R. A. Matzner, R. C. Bales, and J. E. Pemberton, *Appl. Spectrosc.* **48**, 1043 (1994).
13. C. A. Doyle, T. J. Vickers, C. K. Mann, and J. G. Dorsey, *J. Chromatogr. A* **779**, 91 (1997).
14. M. Ho, M. Cai, and J. E. Pemberton, *Anal. Chem.* **69**, 2613 (1997).
15. W. R. Thompson and J. E. Pemberton, *Chem. Mater.* **5**, 241 (1993).
16. W. R. Thompson and J. E. Pemberton, *Chem. Mater.* **7**, 130 (1995).
17. N. J. Harrick, *Internal Reflection Spectroscopy* (Harrick Scientific Corporation, Ossining, New York, 1979).
18. R. P. Sperline, S. Muralidharan, and H. Freiser, *Langmuir* **3**, 198 (1987).

19. J. J. Kellar, W. M. Cross, and J. D. Miller, *Appl. Spectrosc.* **43**, 1456 (1989).
20. D. B. Parry and J. M. Harris, *Appl. Spectrosc.* **42**, 997 (1988).
21. D. B. Parry and J. M. Harris, "Attenuated Total Reflectance FTIR for Measuring Interfacial Reaction Kinetics at Silica Surfaces", in *Chemically Modified Oxide Surfaces*, D. E. Leyden, W. T. Collins, and C. H. Lochmüller, Eds. (Gordon and Breach, New York, 1990), pp. 127–136.
22. S. J. Hug and B. Sulzberger, *Langmuir* **10**, 3587 (1994).
23. P. A. Connor, K. D. Dobson, and A. J. McQuillan, *Langmuir* **11**, 4193 (1995).
24. L. Han, T. M. Niemczyk, Y. Lu, and G. P. Lopez, *Appl. Spectrosc.* **52**, 119 (1998).
25. R. P. Sperline, Y. Song, and H. Freiser, *Langmuir* **8**, 2183 (1992).
26. R. P. Sperline, Y. Song, and H. Freiser, *Langmuir* **10**, 37 (1994).
27. R. P. W. Scott and P. Kucera, *J. Chromatogr.* **149**, 93 (1978).
28. W. B. Lacy, L. Olson, and J. M. Harris, *Anal. Chem.*, paper in revision.
29. R. L. Snyder and P. Poppe, *J. Chromatogr.* **184**, 363 (1980).
30. R. P. W. Scott, *J. Chromatogr. Sci.* **18**, 297 (1980).
31. R. P. W. Scott and P. Kucera, *J. Chromatogr.* **171**, 37 (1979).
32. N. R. Draper and H. Smith, *Applied Regression Analysis* (John Wiley and Sons, New York, 1981), 2nd ed., Chap. 2.
33. A. L. Wong and J. M. Harris, *Anal. Chem.* **61**, 2315 (1989).
34. J. A. Nelder and R. Mead, *Comput. J.* **7**, 308 (1965).
35. T. G. Goplen, D. G. Cameron, and R. N. Jones, *Appl. Spectrosc.* **34**, 657 (1980).
36. H. R. Philipp, *J. Appl. Phys.* **50**, 1053 (1979).
37. R. P. Sperline, S. Muralidharan, and H. Freiser, *Appl. Spectrosc.* **40**, 1019 (1986).
38. E. D. Palik, *Handbook of Optical Constants of Solids* (Academic Press, Orlando, Florida, 1985).
39. N. B. Colthup, L. H. Daly, and S. E. Wiberley, in *Introduction to Infrared and Raman Spectroscopy* (Academic Press, New York, 1990), 3rd ed.
40. D. Lin-Vien, N. B. Colthup, W. G. Fateley, and J. G. Grasselli, *The Handbook of Infrared and Raman Characteristic Frequencies of Organic Molecules* (Academic Press, San Diego, California, 1991).
41. L. R. Snyder, *Principles of Adsorption Chromatography* (Marcel Decker, New York, 1968).
42. W. M. Doyle, *Appl. Spectrosc.* **44**, 50 (1990).
43. I. Langmuir, *J. Am. Chem. Soc.* **40**, 1361 (1918).
44. D. F. Eaton, *Pure Appl. Chem.* **62**, 1631 (1990).
45. A. N. Frumkin, *Z. Phys. Chem.* **116**, 466 (1925).
46. L. R. Snyder and H. Poppe, *J. Chromatogr.* **184**, 363 (1980).